Environmental Science & Technology

Article

pubs.acs.org/est

Resistance of Echovirus 11 to ClO_2 Is Associated with Enhanced Host Receptor Use, Altered Entry Routes, and High Fitness

Qingxia Zhong,[†] Anna Carratalà,[†] Hyunjin Shim,[‡] Virginie Bachmann,[†] Jeffrey D. Jensen,[‡,§] and Tamar Kohn*[,†]

[†]Laboratory of Environmental Chemistry, School of Architecture, Civil and Environmental Engineering, École Polytechnique Fédérale de Lausanne (EPFL), CH-1015 Lausanne, Switzerland

[‡]Jensen Lab, School of Life Sciences, EPFL, CH-1015 Lausanne, Switzerland

Supporting Information

ABSTRACT: Waterborne viruses can exhibit resistance to common water disinfectants, yet the mechanisms that allow them to tolerate disinfection are poorly understood. Here, we generated echovirus 11 (E11) with resistance to chlorine dioxide (ClO_2) by experimental evolution, and we assessed the associated genotypic and phenotypic traits. ClO_2 resistance emerged after E11 populations were repeatedly reduced (either by ClO_2-exposure or by dilution) and then regrown in cell culture. The resistance was linked to an improved capacity of E11 to bind to its host cells, which was further attributed to two potential causes: first, the resistant E11 populations possessed mutations that caused amino acid substitutions from ClO_2-labile to ClO_2-stable residues in the viral proteins, which likely increased the chemical stability of the capsid toward ClO_2. Second, resistant E11 mutants exhibited the capacity to utilize alternative cell receptors for host binding. Interestingly, the emergence of ClO_2 resistance resulted in an enhanced replicative fitness compared to the less resistant starting population. Overall this study contributes to a better understanding of the mechanism underlying disinfection resistance in waterborne viruses, and processes that drive resistance development.

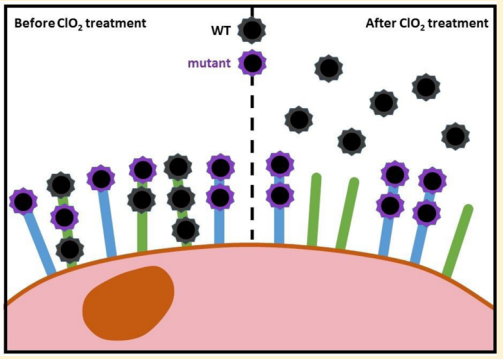

INTRODUCTION

A disinfection step in the water treatment processes constitutes an essential barrier to the transmission of waterborne pathogens. A challenge arises when, despite disinfection, pathogens are not adequately inactivated during water treatment. Incomplete disinfection may result from many different factors, including short-circuiting in the disinfection tank,[1] shielding of the pathogens by particles,[2,3] or a high disinfectant demand of the matrix.[4] Alternatively, the ability to resist disinfection may be a pathogen-inherent trait that may be selected for during the disinfection process. In support of this notion, several studies have reported on the presence of chlorine-resistant microbes in disinfected drinking water.[5−8] To date, however, information regarding the emergence of pathogens resistant to disinfectants remains scarce.

Compared to other pathogens, single-stranded (ss) RNA viruses may be particularly prone to develop disinfection resistance. Because they do not possess proof-reading mechanisms,[9] ssRNA viruses exhibit high mutation rates,[10−12] which enable them to evolve and adapt rapidly to new environments. For example, populations of ssRNA viruses have been reported to readily adapt to stressors such as heat or free chlorine.[13,14]

In previous work, we determined that bacteriophage MS2, a commonly used surrogate for human enteric viruses, can evolve resistance toward chlorine dioxide (ClO_2), and we described the associated resistance mechanisms.[15] Herein, we explore if similar resistance development can also occur in a human pathogenic virus, echovirus 11 (E11). Echovirus, together with coxsackievirus, rhinovirus, poliovirus and enterovirus, belongs to the *Enterovirus* genus of the family *Picornaviridae*. Infective enteroviruses are commonly present in raw wastewater up to 10^3 plaque forming units/L,[1] and there is ample evidence demonstrating that certain enteroviruses can withstand wastewater treatment.[16−19] Moreover, enteroviruses were also detected in finished drinking water and drinking water sources.[20−23] This prevalence of enteroviruses is problematic, because infection by human enteroviruses can lead to serious illness, especially in infants and in immunocompromised individuals.

The structure of the different enteroviruses, including echoviruses, is relatively simple and well-investigated, whereas there are still gaps in the understanding of their complex replication cycle.[24] In brief, enteroviruses are naked, icosahedral viruses with a diameter of approximately 30 nm and a single-stranded, positive sense RNA genome of approximately 7400 nucleotides. The main building block of the enterovirus capsid

Received: June 28, 2017
Revised: August 17, 2017
Accepted: August 24, 2017
Published: August 24, 2017

DOI: 10.1021/acs.est.7b03288
Environ. Sci. Technol. 2017, 51, 10746−10755

is a protomer that contains viral proteins (VP) 1−4, whereby the structural differences in the loops of VP1-VP3 give each type of enterovirus its distinct morphology and antigenicity.[25] The enterovirus surface has an uneven topography, with a plateau at the 5-fold axis surrounded by a deep depression (canyon) and another high point at the 3-fold axis (Figure 1).

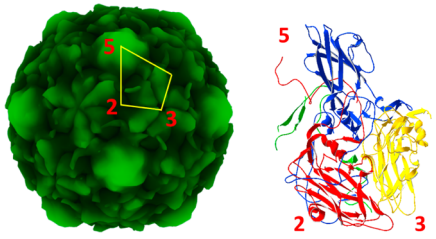

Figure 1. Echovirus 11 capsid topography and protein protomer. Left: Surface rendering of the half capsid of an echovirus 11 with radial coloring showing the relative distance from the center of the particle. Darker regions are closer to the particle center. The 2-fold, 3-fold, and 5-fold symmetry axes are labeled in red. The location of one protomer is indicated in yellow. The image was produced in Chimera based on PDB entry 1H8T.[75] Right: The protomer composed of VP1 (blue), VP2 (yellow), VP3 (red), and VP4 (green) with the symmetry axes labeled. The canyon, which is a deep depression surrounding the 5-fold axis is formed by VP1 and VP3, and is recognized as a receptor-binding site for some other enteroviruses.[25] The structure was visualized by Swiss-PdbViewer based on PDB entry 1H8T.[75]

As a primary host cell receptor, echovirus 11 uses cell surface protein decay-accelerating factor (DAF or CD55).[26] To trigger entry into the host, the virus must additionally interact with secondary or coreceptors, such as β2-microglobulin.[27−29] Host entry can occur by different endocytic mechanisms, including clathrin- and caveolin-mediated endocytosis, as well as macropinocytosis.[30−33] After entry, membrane vesicles carrying viruses move in the cytoplasm with the aid of microtubules or actin to the endosome where uncoating occurs. The genome is then translated in the cytoplasm into a single polyprotein which is split into four structural proteins (VP1−4) and seven nonstructural proteins ($2A^{pro}$, 2B, 2C, 3A, 3B, $3C^{pro}$, and $3D^{pol}$).[34] The subsequent genome replication occurs in double membrane vesicles in the cytoplasm. Finally, new virions are released from the cell via lysis.

During disinfection, viruses are damaged such that one or several steps in their replication cycle can no longer be completed, resulting in inactivation. ClO_2 is a highly effective disinfectant which has been shown to inactivate a broad range of viruses including feline calicivirus, hepatitis A virus, coxsackievirus, adenovirus, poliovirus and rotavirus.[35−38] The virucidal mechanism of ClO_2 appears to differ between viruses: in bacteriophage MS2, the mode of action of ClO_2 mainly involves the degradation of the viral proteins, which in turn impairs the viral binding to host cells.[39] In enteroviruses, in contrast, ClO_2 has been proposed to act on the viral genome. Specifically, it was suggested that inactivation of poliovirus, enterovirus 71 and hepatitis A virus by ClO_2 were caused by damage in the 5′ noncoding region.[40−43] It was, however, not resolved if genome damage fully accounts for the observed infectivity loss, or if protein damage also contributes to inactivation. For example, Li et al. suggested that the destruction of antigenicity was partly responsible for the inactivation of hepatitis A virus.[40] Similarly, Simonet and Gantzer observed a discrepancy between poliovirus infectivity loss obtained by cell culture and genome decay measured by real-time PCR, suggesting an important role of protein damage in inactivation.[42] In contrast, Alvarez and O'Brien also observed reaction of ClO_2 with the capsid of poliovirus, but reported that the critical target was viral RNA.[44] Given the range of viral components and functions targeted by ClO_2, ClO_2-resistance in echovirus may thus result from modification to any of the major viral functions (host binding, host entry or genome replication).

The objectives of this study were to determine genotypic and phenotypic characteristics associated with E11 resistance to ClO_2. Specifically, we first developed E11 with resistance to ClO_2 by experimental evolution and identified the accompanying genotypic modifications. We then assessed which viral functions are altered in resistant viruses and evaluated the cost of acquiring resistance with respect to the virus' replicative fitness.

EXPERIMENTAL SECTION

Cells and Viruses. Details pertaining to the culturing, purification and enumeration of E11 and associated host cells are given in the Supporting Information (SI).

Chlorine Dioxide Production. Concentrated ClO_2 was produced as described previously[15] and was stored in the refrigerator at 4 °C. ClO_2 working solutions were prepared in phosphate-buffered saline (PBS; 5 mM Na_2HPO_4 (99%, Acros), 10 mM NaCl (99.5% (Acros), pH 7.4) immediately prior to each experiment.

Experimental Evolution Assays. Experimental evolution assays to produce ClO_2-resistant E11 were conducted analogously to those described previously for MS2 coliphage.[15] In brief, a commercially available starting population of E11, hereafter referred to as "wild-type" (WT) was subjected to repeated cycles of ClO_2 exposure. Following inactivation, the remaining infective viruses were concentrated, washed with PBS, and were spiked onto a monolayer of BGMK cells. The multiplicity of infection (MOI) was less than 0.005 (approximately 10^2−10^4 viruses, quantified as most probable number cytopathogenic units (MPNCU), per 2.6×10^6 cells). After incubation at 37 °C, the regrown populations were purified as described in the SI, and re-exposed to ClO_2. The disinfection-regrowth cycles were conducted until cycle 10, when the evolved population was divided and two experimental evolution assays were continued in parallel with ten more cycles. After a total of 20 cycles, an approximately 50% reduction in inactivation rate constant by ClO_2 was achieved (see below) and the experiment was halted. The two resulting populations are named EA and EB hereafter, where E stands for "exposed to ClO_2". The ClO_2 concentration used was 0.5 mg/L in the early cycles, and incrementally increased to 4 mg/L at cycle 15 and following.

Our previous work on MS2 revealed that resistance to ClO_2 could emerge if MS2 populations were repeatedly subjected to sharp reduction in size (bottleneck event) and then regrown, whereby the cause of the bottleneck (ClO_2 or dilution) was irrelevant.[15] We therefore included two E11 populations in this study, which were repeatedly subjected to bottleneck events induced by dilution rather than ClO_2 exposure, followed by regrowth in cell culture. Specifically, after each regrowth step, the populations were diluted and approximately 10^2−10^3 MPNCU were passed to the next cycle. The dilution-regrowth cycles were continued for 10 cycles, at which point a comparable extent of resistance as in populations EA and EB

DOI: 10.1021/acs.est.7b03288
Environ. Sci. Technol. 2017, 51, 10746−10755

was achieved. The two resulting populations are henceforth named NEA and NEB, where NE stands for "non-exposed".

Kinetic Inactivation Experiments with ClO_2. To monitor the emergence of ClO_2 resistance, the rate constants for the inactivation of the evolved E11 populations by ClO_2 were compared to those of the wild-type. To this end, E11 was spiked into beakers containing 2 mL PBS to a starting concentration of approximately 10^8 MPNCU/mL. The reactors were then spiked with a one-time dose of ClO_2 to yield an initial concentration of 1 mg/L. All the experiments were conducted in 10 mL beakers positioned on ice, and reactors were continuously stirred. Samples were taken periodically and mixed immediately with PBS containing 10% w/v sodium thiosulfate (98%, Sigma-Aldrich) to quench the residual ClO_2. To derive kinetic parameters, inactivation data of replicate experiments were pooled and fitted to the modified Hom model, which accounts for the fact that the ClO_2 concentration decayed over time:[45]

$$\ln\frac{N}{N_0} = -k_{ClO2}C_{ClO2,0}^{n}t^{m}\left(\frac{1-\exp\left(-\frac{k_d t}{m}\right)}{\frac{k_d t}{m}}\right)^{m} \quad (1)$$

Here N and N_0 are the infective virus concentrations at times t and 0 respectively; C_0 is the initial ClO_2 concentration, k_{ClO2} the Hom inactivation rate constant $[(mg/L)^{-n}min^{-m}]$, m is a parameter that describes the deviation from first-order, n is the coefficient of dilution, and k_d $[min^{-1}]$ is the decay rate constant of ClO_2. The concentration of ClO_2 (C) was measured throughout the experiments by mixing sample aliquots at a 1:2 molar ratio with chlorophenol red (Sigma) and spectrophotometrically measuring its discoloration.[46] The value of k_d (0.11−1.10 min^{-1}) was then determined from a first-order fit of the ClO_2 concentration versus time:

$$\ln\left(\frac{C}{C_0}\right) = -k_d t \quad (2)$$

As specified previously,[15] parameters m and n were treated as constant parameters across all experiments and were determined for each virus by simultaneously fitting all the experiments conducted while varying only k_{ClO2}. The values of m and n correspond to 0.30 and 0.46 respectively.

For ease of readability, inactivation data is presented as plots of $\log_{10}$ inactivation $\left(\log_{10}\left(\frac{N}{N_0}\right)\right)$ versus ClO_2 exposure. Hereby the exposure corresponds to the (time-dependent) concentration of ClO_2, integrated over the exposure time t:

$$ClO_2 exposure = \int_0^t C dt \quad (4)$$

Viral Genome Characterization. The whole genomes of virus populations of interest were interrogated by Next Generation Sequencing (NGS). The NGS data were further used to identify mutation clusters. In addition, the ratios of nonsynonymous or synonymous segregating sites (pN/pS) were calculated for each protein-coding gene of the evolved populations, in order to characterize the genomic response of different proteins to the imposed experimental conditions. BLAST analysis was performed using Geneious (Version 10.0.8) to compare the genome sequences of the evolved populations with published sequences. Experimental and computational details pertaining to the genome characterization are given in the SI.

Quantification of Host Binding. The ability of E11 to bind to host cells was assessed either by quantifying the host cells exhibiting attached viruses, or by enumerating the viruses bound to cells.

To measure the number of cells with bound viruses, a flow cytometry assay was modified from Triantafilou et al.[47] Specifically, cells were harvested using 1:10 diluted citric saline solution (concentrated solution: 1.35 M KCl (Acros) and 0.15 M $NaC_6H_7O_7$ (Sigma)) and fixed in fixing buffer (4% paraformaldehyde; AlfaAesar) for 10 min on ice, followed by washing with PBS supplemented with 30 mM glycine (Sigma) and blocking buffer (PBS with 1% bovine serum albumin (Sigma)). Cells were incubated in 1 mL blocking buffer for 30 min at room temperature, and were then counted to ensure the presence of roughly 10^6 cells/mL. E11 diluted in binding buffer (PBS supplemented with 2 mM $CaCl_2$ (99+%, Acros) and 1 mM $MgCl_2$ (99%, Acros) was added to the cells and incubated for 1 h at room temperature. Care was taken to use the same MOI for samples that were directly compared. After incubation, unbound viruses were removed by washing three times in binding buffer. Cells were then sequentially incubated on a rotator with a primary anti-E11 mouse monoclonal antibody (LSBio) and secondary goat antimouse antibody conjugated with FITC (Sigma), at a concentration of 5 μg/mL each. Between each incubation with antibody, cells were washed three times with blocking buffer. Staining was measured using a CyFlowSL flow cytometer (Partec) and analyzed by FlowMax (see SI, Figure S1). To test the role of the DAF receptor in host binding, cells were incubated with rabbit monoclonal anti-DAF antibody conjugated with APC (Biorbyt) at a concentration of 20 μg/mL to block the receptors prior to exposure to the virus.

To quantify the number of viruses attached to cells, an approach based on cell culturing was used. Viruses were incubated with cell monolayers on 6-well plates for 1 h on ice. The cell monolayer was then washed with PBS to remove any unbound virus. Trypsin-EDTA (Gibco, Frederick, MD) solution was used to detach the cell monolayer. Cells were then subjected to chloroform treatment as described in the virus production procedure (SI) and the virus was harvested and quantified by quantitative real-time PCR (qRT-PCR) as described in the SI.

Assessment of Receptors and Entry Routes Used. To identify the key attachment and entry routes, viral growth curves of the populations of interest were compared under three conditions: standard growth conditions in BGMK cells; growth on cells pretreated with anti-DAF antibody to block the primary cell receptor; and growth of viruses in the presence of drugs that inhibit different attachment or entry routes. Details pertaining to each condition are given in the SI.

Competitive Fitness. The replicative fitness of the mutants was assessed in competition with the wild-type. Specifically, a mutant population (EA or NEA) was coinfected with WT onto BGMK, A549, Vero or Caco-2 cell lines at a 1:1 ratio. To identify the virus with the greater fitness, the WT:mutant ratio was reassessed 72 h post infection. To do so, genome segments 5061−5354 and 6895−7193 were Sanger sequenced using primer sets 20 and 27 (SI, Table S1) for EA and NEA, respectively (see SI for details). These two segments contain one mutation each (T5203C and A6989G) that is present in <2% of the WT but in >95% of the mutant, and thus allow to distinguish between WT and mutant. The sequencing peak

DOI: 10.1021/acs.est.7b03288
Environ. Sci. Technol. 2017, 51, 10746−10755

height of WT and the mutants at the two mutation sites was used to evaluate the WT:mutant ratio at the time of coinfection and 72 h post infection. While this approach is only semiquantitative, it allowed us to determine which virus prevailed in direct competition.

Statistical Analysis. The goodness-of-fit of the data was evaluated based on the coefficient of determination (R^2) determined by GraphPad Prism (Version 6.01, 2012). Likelihood ratio (LR) test[48] was applied to determine if the inactivation kinetics significantly differed between two or more viral populations, with the threshold p-value for statistical significance, determined by Chi-squared test, set to 0.05. Unpaired t test or regular one-way ANOVA was applied to compare all other parameters between populations.

Accession Numbers. Genome sequence obtained by NGS of the WT, EA, EB, NEA and NEB populations have been deposited in NCBI's BioSample database with the accession numbers SAMN07510747 to SAMN07510751.

RESULTS AND DISCUSSION

Emergence of Resistance. Pooled inactivation curves of WT and the resistant (or mutant) populations E and NE are shown in Figure 2A. The curves exhibit a tailing feature that is

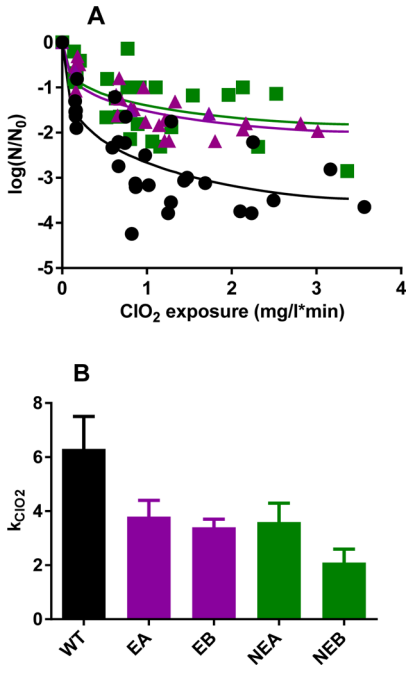

Figure 2. Disinfection kinetics of E11 by ClO_2. (A) Inactivation data of E11 WT (black circles), E (purple triangles) and NE (green squares) are shown as filled symbols. Solid lines indicate the corresponding fits to the modified Hom Model (eq 1). (B) Inactivation rate constants k_{ClO2} of the wild-type and the four evolved populations EA, EB, NEA, and NEB at their final passages.

frequently observed for virus inactivation by ClO_2.[36,41,49] This behavior is well-captured by the modified Hom model (eq 1). Despite some scatter in the data, it is apparent from Figure 2A that both the exposed populations and the nonexposed echovirus populations were more resistant to ClO_2 than WT. Figure 2B shows the inactivation rate constants of WT and all evolved populations. ClO_2-resistance in the evolved populations is manifested in values of k_{ClO2} that were significantly smaller than that of WT ($p < 0.01$ for all four populations). The k_{ClO2} of the evolved populations ranged from 33% to 60% of that of WT.

Similar to our previous observation on the emergence of ClO_2 resistance in MS2,[15] viruses evolved from both ClO_2-exposed and nonexposed evolution pathways became resistant to ClO_2. This finding may be explained by two effects: first, it is known that serial passages of viruses in cells can lead to an increased replicative fitness as a result of cell culture adaptation.[50,51] Repeated viral regrowth in our experimental setup could thus intensify the selection of adapted viruses with a replicative advantage. Second, the repeated bottleneck events likely promoted those E11 variants that most successfully regrew from low MOI, and the traits that allow for efficient regrowth may also be essential for ClO_2 resistance. Overall, we thus suggest that, analogous to ClO_2 resistance in MS2, it was repeated regrowth from a population bottleneck that induced ClO_2 resistance in E11. In contrast, we are not able to identify the role of ClO_2 exposure as a sole or additional driving force that induced the resistance.

Genotypic Features of Resistant Populations. Next generation sequencing was utilized to identify the genomic changes related to resistance. Mutations in the evolved final populations were identified with reference to the WT consensus sequence and are shown in Table 1. This table includes all mutations that changed from minor to major alleles, as well as those that changed from major (50−98%) to fixed (>99%) alleles. The identified mutations were located in both

Table 1. Heat Map of the Frequency of Alleles That Changed from Minor to Major or from Major to Fixed in the Evolved Populations EA, EB, NEA, and NEB, Compared to the Wild-Type WT, As Identified by Next Generation Sequencing[a]

0 50 100%

	Nucleotide	Amino acid	WT	EA	EB	NEA	NEB
VP2	G1373C[c]	G139R	63	**100**	**99**	**100**	**100**
VP3	A1761T	N6I	<1	<1	<1	**98**	**99**
VP1	A2835G	K126R	6	61	65	<1	<1
	C2844A[b]	P129Q	24	63	68	<1	<1
	T2849A	S131N	6	60	65	<1	<1
	C2850A	S131N	6	60	65	<1	<1
	A2937T[b]	Y160F	<1	<1	<1	**99**	**99**
	C3101A[b]	H215N	<1	<1	<1	**99**	**99**
	C3162T	T235I	10	63	66	<1	<1
	A3170G	M238V	3	63	66	<1	<1
	A3233G	K259E	6	63	65	<1	<1
2C	G4384A	/	30	98	**99**	<1	<1
	A4552G	/	4	97	98	<1	<1
3A	T5203C	/	<1	97	96	<1	<1
	T5323C	/	46	69	43	61	51
3B	G5389A	/	3	<1	69	<1	<1
$3C^{pro}$	C5650T	/	<1	3	85	<1	<1
	T5788A	/	<1	97	97	<1	<1
	A5893T	/	7	97	98	<1	<1
$3D^{pol}$	T6006C	M19T	37	98	**99**	<1	<1
	C6006T[c]	T19M	63	2	1	**100**	**100**
	C6061T	/	7	97	98	<1	<1
	G6409A	/	16	95	97	<1	<1
	T6562C	/	33	97	98	12	<1
	C6562T[c]	/	67	2	2	88	**100**
	C6586T[d]	/	7	<1	50	<1	<1
	C6745T	/	<1	69	<1	<1	<1
	A6989G	T347A	2	1	3	97	98
3'-UTR	G7383A	/	2	67	3	<1	1

[a]The location of the mutation, and the resulting change in nucleotide and amino acid are listed. Mutations that reached fixation (≥99%) are indicated by bold fonts. [b]These mutations on the structural protein VP1 caused an amino acid substitution from ClO_2-reactive to nonreactive ones. [c]At these locations, major alleles in WT became fixed in some evolved populations. The change from WT to evolved population thus concerns the mutation of the minor WT allele to the major one. In these cases, the notation therefore indicates the minor allele (or amino acid) of the WT on the left, and the major or fixed one on the right. [d]At this location, EB has 50% C and 50% T.

DOI: 10.1021/acs.est.7b03288
Environ. Sci. Technol. 2017, 51, 10746−10755

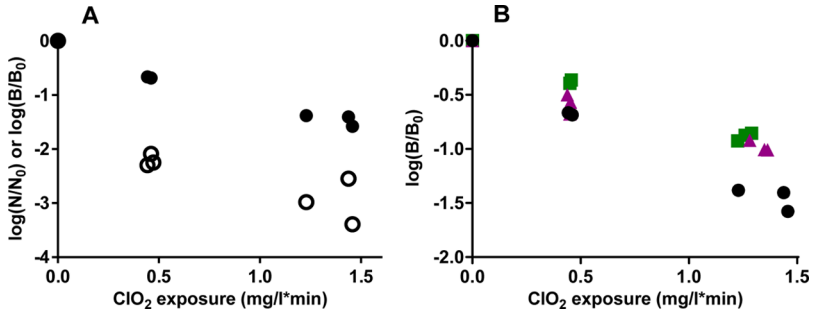

Figure 3. Effect of ClO_2 on virus binding to host cells. (A) Infectivity loss (open circles) and binding loss (filled circles) of WT as a function of ClO_2 exposure. N/N_0 indicates the proportion of infective viruses measured by culturing. B/B_0 indicates the proportion of cells with bound viruses, measured by flow cytometry. (B) Comparison of the binding loss as a function of ClO_2 exposure among wild-type (black circles), EA (purple triangles) and NEA (green squares).

structural and nonstructural proteins, while most nonsynonymous mutations were in the structural proteins. Both synonymous and nonsynonymous mutations can cause phenotypic changes in enteroviruses, but these effects are more common for nonsynonymous mutations.[52] Therefore, nonsynonymous mutations are more likely to be involved in adaptation to disinfection.

The final E and NE populations exhibited very distinct sets of mutations, despite their similar resistance to ClO_2 (Figure 2). The mutations found in the E but not NE populations may be a result of adaptation of E to ClO_2. Alternatively, the differences in mutational spectra may stem from the different numbers of experimental evolution passages experienced by the two population types (10 for NE versus 20 for E). Within each population type, the replicates had similar genotypes. Replicates EA and EB shared most of their mutations, including nine synonymous changes. Populations NEA and NEB exhibited the same consensus sequence.

Of the mutations listed in Table 1, several emerged in clusters (see SI, Table S2 and accompanying text for details). The clustering of mutations suggests that while certain allele frequencies may be rising owing to genetic hitchhiking,[53] one or more mutations in each cluster are likely a result of positive selection.[54] Yet, a comparison of the ratio of nonsynonymous to synonymous polymorphism (pN/pS) across proteins yielded pN/pS ratios <1 for all proteins and virus populations (SI Table S3), indicating strong purifying selection. This observation is consistent with the small number of mutations being fixed during the experiment.

Role of Host Binding in Inactivation and Resistance. Resistance to ClO_2 implies that the majority of viruses in the population can execute their essential functions—host binding, entry, replication and assembly—despite exposure to ClO_2. For wild-type MS2, we previously demonstrated that ClO_2 impairs host binding,[39] while ClO_2-resistant MS2 are able to better maintain host binding in the presence of ClO_2.[15] It is conceivable that a similar mechanism underlies echovirus resistance to ClO_2. This notion is supported by our finding that positively selected mutations mainly occurred in the structural proteins (Table 1) which are related to host attachment and entry.

To test the role of host binding in resistance development, we first confirmed that the inactivation of E11 WT coincides with a loss in host binding (Figure 3A). We then compared host binding in the presence of ClO_2 between the WT and that of the evolved populations (Figure 3B). As observed for MS2, the effect of ClO_2 on host binding was diminished for E and NE at any given ClO_2 exposure. Overall, the two evolved populations exhibited lower binding loss rates than WT (p-values of 0.025 and 0.020 respectively). This finding suggests that an enhanced binding capacity of echovirus to the host cells contributes to the observed ClO_2 resistance.

Protein Modifications Associated with Enhanced Host Binding. The differences in host binding between mutants and WT could be tentatively linked to the genetic and associated protein modifications in the evolved populations. For this analysis, we relied on literature reports of the same or similar mutations, as well as on chemical and structural considerations. E11 uses DAF as the main cellular receptor,[26] and various binding sites on E11 to DAF have been suggested. Stuart et al. postulated that the binding site is located close to 5-fold axis (Figure 1),[55] whereas Rezaikin et al. argued that it is near the 2-fold axis, as encountered in many other enteroviruses.[56] In addition, both studies suggested the presence of an alternative unidentified coreceptor which binds in the canyon region, a depression surrounding the 5-fold axis formed by VP1 and VP3 (Figure 1).

Of the 14 nonsynonymous mutations listed in the mutant populations, 11 are located on structural proteins VP1, VP2, and VP3 (depicted in SI Figure S4). In the mutant E populations, a series of mutations (S131N, P129Q, K126R, T235I, and M238V) line the canyon wall on VP1 (SI Figure S4). The cellular receptor DAF binds away from the canyon across VP2 and VP3. As such, it is unlikely to be affected by the mutations on the canyon wall. However, the interaction between E11 and DAF have a low affinity while the interaction between poliovirus and rhinovirus with their corresponding canyon-binding receptors PVR and ICAM-1 are higher.[57−59] It is thus conceivable that the series of VP1 mutations along the canyon wall enhances the interaction between the virus and an unknown canyon-binding (co)receptor and strengthen virus binding in the canyon relative to DAF. This, in essence, would constitute a shift in the main cellular receptor used by ClO_2-resistant echovirus. Previous studies confirm that echovirus can use the canyon region for receptor binding. For example, echovirus 1 uses the canyon region for binding to the functional domain $\alpha 2I$ of human $\alpha 2\beta 1$.[31]

A shift in the cellular receptors is further supported by comparing the mutations found herein with those previously found in variants of E11 with altered cell receptor use. Stuart et al. identified a number of mutations present in a variant of E11 that was able to infect cells in a DAF-independent manner.[55] Specifically, the DAF-independent echovirus had mutations in location 139 on VP2, alongside seven others including position

DOI: 10.1021/acs.est.7b03288
Environ. Sci. Technol. 2017, 51, 10746−10755

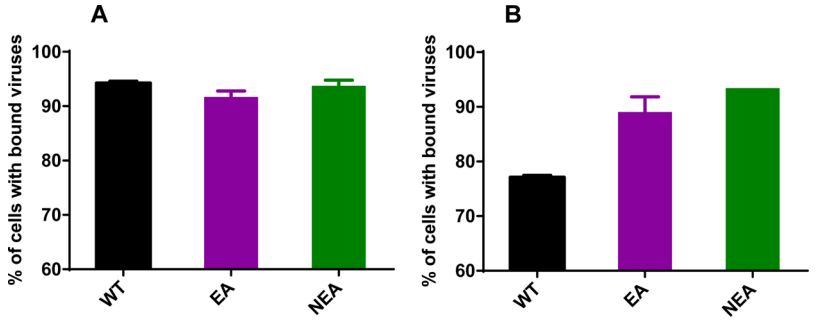

Figure 4. Comparison of the binding efficiency of the wild-type and the mutant populations EA and NEA on BGMK cells (A) in the absence and (B) in the presence of anti-DAF antibodies. The results are presented as the percentage of virus-positive cells measured by flow cytometry. The error bars represent the range of two replicates.

132, 240, and 259 in the canyon region of VP1. Site 139 was also highlighted by others, who recognized it to be an important site for poliovirus interaction with its canyon-binding receptor PVR.[60,61] The E populations described herein also contain mutations in positions 139 and 259 (G139R in VP2 and K259Q in VP1). Although arginine was already the major allele in WT at position 139, it became fixed in all the evolved populations, and therefore is potentially beneficial in our experimental setup. Additionally, mutations S131N and M238V in the E populations are situated close to mutations at positions 132 and 240 identified by Stuart et al. Rezaikin et al. determined that a mutation at position 129 was related to altered cell tropism in E11.[56] A mutation in this position, P129Q, was also found in the E populations. Notably, this mutation also caused the substitution of a ClO_2-reactive amino acid (proline) by a ClO_2-stable one (glutamine). This suggests that this mutation renders the protein capsid more enduring when exposed to ClO_2, which may contribute to the mutant's enhanced ability to bind in the presence of ClO_2.

NE populations, on the other hand, have only four mutations on the structural proteins (depicted in SI Figure S4B). Mutation G139R on VP2 was shared with E populations, and its role in altering cell receptor use was discussed above. Mutation H215N is positioned in the binding region of coxsackievirus B3 with its canyon-binding receptor.[62] Strauss et al. observed a conformational change in the corresponding site of poliovirus when the virus bound to the canyon-binding receptor PVR.[60] This suggests that position 215 on VP1 is linked to usage of a canyon-binding receptor in other enteroviruses, and E11 may also exploit this alternative. Finally, this mutation, along with mutation Y160F, substitute ClO_2-labile by ClO_2-stable amino acid residues, thereby enhancing the chemical capsid stability of the NE populations compared to WT.

Experimental Evidence for Alternative Receptor Use by Resistant Populations. To experimentally confirm that ClO_2-resistance altered the receptor use of populations E and NE, the binding ability of the different virus populations to BGMK cells was quantified while partly blocking cellular receptor DAF by anti-DAF antibodies. Results showed that all the viruses bound equally well to BGMK cells in the absence of anti-DAF antibodies (Figure 4A and SI Figure S2). This result was anticipated because the mutations identified on the viral structural protein were not located within binding sites to DAF, and hence the interaction between virus and this receptor was not affected. However, when anti-DAF antibodies were added and DAF was less accessible, mutant populations still successfully bound to BGMK, whereas the proportion of virus-bound cells decreased significantly for WT populations ($p = 0.0008$; Figure 4B and SI Figure S3).

The effect of the anti-DAF antibody was confirmed by comparing growth curves of each virus with or without addition of the antibody (SI Figure S5 and Table S4). With the antibody added, the exponential phase growth rate of WT decreased to 42% of its original value, while EA and NEA retained 71% and 59% of their original growth rate, respectively. The final virus concentration also decreased to 3% of the original concentration for WT, compared to a smaller decrease in EA (10%) and no final titer decrease in NEA.

Finally, changes in receptor use were also supported by testing the virus' susceptibility to pleconaril. This antipicornavirus drug induces a conformational change in the floor of the canyon, which in turn blocks receptor binding and/or the uncoating process.[63] The growth of EA and NEA was completely inhibited in the presence of 1.3 μM pleconaril (SI Figure S6A and B), while WT increased in titer after 12 h of incubation with host cells (SI Figure S6B). Two possible explanations can be invoked to explain these results. First, as discussed above, E and NE may use the canyon as a binding motif, and hence may be more strongly affected by a drug affecting the canyon confirmation. Alternatively, the mutant populations may have stronger interactions with pleconaril compared to the WT. Interestingly, previous studies on the effect of pleconaril on enteroviruses, including E11, showed that the presence of valine in the hydrophobic pocket region of the canyon was associated with increased pleconaril susceptibility, whereas methionine impeded pleconaril insertion.[64−66] This is thus consistent with the mutation M238V of E populations rendering them more susceptible to pleconaril.

Combined, these results are consistent with the hypothesis that the ClO_2-resistant mutants developed the capacity to better utilize an alternative canyon-binding cellular receptor compared to the WT, which ultimately allowed them to better bind to host cells after treatment by ClO_2.

Entry Routes Altered by ClO_2-Resistance. Besides altering cellular receptor requirements, the mutations in E and NE may change viral entry routes, which are linked to receptor use.[67,68] Here, we used a suite of drugs that inhibit different cellular factors linked to endocytosis (SI Table S5), to identify if ClO_2 resistance altered the role of these endocytosis markers. Specifically, different entry steps in WT and mutants were probed using nystatin, chlorpromazine, cytochalasin D, nocodazole, and rottlerin (SI Table S5). Nystatin sequesters choresterol and thus targets the caveolin-mediated entry route, which involves cholesterol rich membranes.[33,69] Nystatin did not have any effect on cell infection and growth of WT, but

DOI: 10.1021/acs.est.7b03288
Environ. Sci. Technol. 2017, 51, 10746−10755

reduced the production of E and NE (Figure 5). This indicates that WT does not enter cells by a caveolae-mediated route,

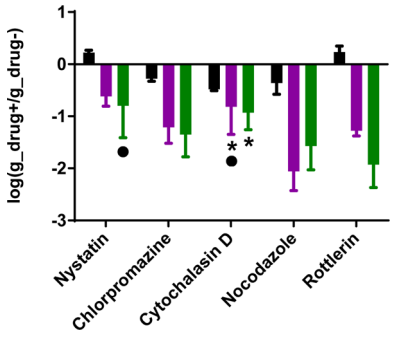

Figure 5. Effect of various entry inhibitors on infection of BGMK cells by WT (black), EA (purple) and NEA (green). The number of genome copies after 12 h of incubation in the presence of a drug (g_drug+) was determined by qRT-PCR and compared with that in the drug-free controls (g_drug-). The error bars represent standard deviations of triplicate experiments. ●: the inhibition effect by adding the drug is not significant ($p > 0.05$); *: Inhibition in growth is not significantly different between WT and mutant ($p > 0.05$). The concentrations of the drugs were: Nystatin, 50 μM; Chlorpromazine, 40 μM; Cytochalasin D, 8 μM; Nocodazole, 40 μM; Rottlerin, 10 μM.

whereas this entry route was employed by E and NE. The clathrin-mediated entry route is inhibited by chlorpromazine, which prevents the assembly of clathrin lattices.[30] Chlorpromazine inhibited all viruses, though the effect on the ClO_2-resistant populations was more prominent. Therefore, clathrin-mediated entry might be a minor route for WT whereas the mutants rely more heavily on this route. Cytochalasin D inhibits actin polymerization and, as such, could have an effect on all the membrane trafficking routes as well as macropinocytosis.[70,71] At the added concentrations, cytochalasin D affected the resistant viruses to a seemingly greater extent than the WT though the difference was not statistically significant ($p = 0.078$). Hence the infection of BGMK cells by WT may be less dependent on intact actin, and WT may be less likely to use macropinocytosis as the entry route. The lack of importance of macropinocytosis in the WT was further supported by experiments using rottlerin. Rottlerin inhibits protein kinase C (PKC), which is a stimulant of micropinocytosis.[32] Production of WT was not affected by rottlerin, indicating that disruption of the macropinocytosis entry route was irrelevant for infection by WT. In contrast, both mutants had more than 90% reduction in growth in the presence of the drug. Thus, entry of the mutants are PKC dependent. Upla et al. suggested that PKC activity is needed for the signaling pathway induced by echovirus binding to $\alpha 2\beta 1$ integrin.[72] As proposed above, the mutants potentially use a canyon-binding receptor such as $\alpha 2\beta 1$. The importance of PKC for the mutants but not WT may thus be linked to signaling from $\alpha 2\beta 1$ binding. Finally, upon entry, nocodazole disrupts microtubules that are considered vital for the travel of endosomes to the perinuclear region.[73] Microtubules were vital for successful infection of BGMK cells by the mutants, while WT was only affected to a minor extent. Therefore, WT E11 has a transport system that does not rely on microtubules.

Overall, these results demonstrate multiple effects of resistance development on E11 entry routes. While these changes may be neutral and not directly involved in the mechanism of resistance, they indicate profound alteration of the viral life cycle.

Effect of Resistance on Replicative Fitness. Arguably the most relevant question related to disinfection resistance is whether the resistant mutants can compete with or even outcompete the WT. We therefore tested the fitness of the resistant populations individually and in direct competition with the WT. When each virus population was individually grown on BGMK cells, no significant difference was observed in their growth rate, final titer or genome copy number (SI Figure S7). All virus populations were thus equally fit if grown individually. However, if WT and mutant viruses were coinfected at a 1:1 ratio, the resistant viruses dominated the population after 72 h of growth (SI Figure S8). Similar experiments were repeated in Caco-2, Vero and A549 cell lines (data not shown). With the only exception of Vero cells, where mutant NE populations were equally fit as WT, E and NE were consistently fitter than WT. These results indicate that the fitness advantage of the ClO_2-resistant mutants is not specific to the host cell that they are adapted to. Instead, under our experimental conditions the mutants could outcompete WT in all cell lines tested.

The finding of greater fitness in the evolved populations raises the question of why the associated genetic changes are not already present in the starting population (WT), and if the relevant mutations are encountered in naturally occurring enteroviruses. Compared to experimental evolution, conditions encountered in virus evolution during natural circulation are considerably more complex, and involve both virus transmission via the environment and from person-to-person. Therefore, the beneficial mutations that emerged during experimental evolution may be neutral or even detrimental in the natural environment. Interestingly, a nucleotide BLAST analysis of VP1 revealed that all of the mutations identified in VP1 have previously been reported in clinical or sewage isolates of E11 (SI Table S6). Two mutations C2844A and T2849A were present in more than 98% of the 487 full VP1 sequences included. The other mutations were present at 0.4% to 44.6%. Similarly, a BLAST analysis of VP2, VP3 and $3D^{pol}$, the other proteins with nonsynonymous mutations, revealed previous reports of all but one mutation (C6006T) as well. This indicates that most nonsynonymous mutations identified here are neutral or even beneficial to actual virus circulation, even if they were not acquired by the WT used herein. Ultimately, this implies that viruses with ClO_2 resistance may successfully circulate.

Implications for Virus Disinfection Practice. This work demonstrates that ClO_2-resistant populations of a human pathogenic virus, E11, can emerge as a result of frequent expansion from low population numbers. To date, it remains unclear if resistance develops during natural virus circulation, given that a virus' natural environment is a more complex system involving selection by more diverse stressors compared to the in vitro system considered herein. Even if it evolved naturally, however, resistance may go undetected, as outbreaks of waterborne viral disease are difficult to capture, and because even in the resistant viruses some disinfection susceptibility remains. Nevertheless, this study suggests that viruses can exist that challenge current disinfection practices. Specifically, the US EPA currently suggests a ClO_2 dose of 33.4 mg·min/L to ensure a 4 $\log_{10}$ inactivation of viruses at 5 °C.[74] At this dose, the E11 WT would undergo an inactivation of 8 $\log_{10}$, whereas that of E and NE would only amount to 4 $\log_{10}$. Although the

DOI: 10.1021/acs.est.7b03288
Environ. Sci. Technol. 2017, 51, 10746−10755

inactivation E and NE still falls within the desired range, the discrepancy to the inactivation of the WT highlights that current disinfection protocols and water treatment standards may need to be adapted to ensure the control of resistant viruses and limit their proliferation.

■ ASSOCIATED CONTENT

Supporting Information

The Supporting Information is available free of charge on the ACS Publications website at DOI: 10.1021/acs.est.7b03288.

Additional experimental information on cells and viruses, viral genome sequencing, identification of mutations clusters, *pN*/*pS* analysis, analysis of flow cytometer output, quantitative real-time PCR (qRT-PCR), E11 binding to BGMK cells, growth curves and drug inhibition assays, competitive fitness, and BLAST analysis (PDF)

■ AUTHOR INFORMATION

Corresponding Author

*Phone: +41 21 693 0891; e-mail: tamar.kohn@epfl.ch.

ORCID

Tamar Kohn: 0000-0003-0395-6561

Present Address

§J.D.J.: Jensen Lab, School of Life Sciences, Arizona State University, Tempe, Arizona 85281, United States.

Notes

The authors declare no competing financial interest.

■ ACKNOWLEDGMENTS

This work was funded by the Swiss National Foundation (project numbers 31003A_138319 and 31003A_163270). HS was supported by a European Research Council (ERC) Starting Grant to JDJ. We thank Philippe Jacquet for help with the analysis of the NGS data.

■ REFERENCES

(1) Hewitt, J.; Leonard, M.; Greening, G. E.; Lewis, G. D. Influence of wastewater treatment process and the population size on human virus profiles in wastewater. *Water Res.* **2011**, *45* (18), 6267−6276.

(2) Winward, G. P.; Avery, L. M.; Stephenson, T.; Jefferson, B. Chlorine disinfection of grey water for reuse: Effect of organics and particles. *Water Res.* **2008**, *42* (1−2), 483−491.

(3) Stewart, M. H.; Olson, B. H. Bacterial resistance to potable water disinfectants. In *Modeling Disease Transmission and Its Prevention by Disinfection*; Cambridge University Press: Cambridge, 1996; pp 140−192.

(4) *Environmental Microbiology*, 3rd ed..; Pepper, I. L., Gerba, C. P., Gentry, T. J., Maier, R. M., Eds.; Elsevier Inc.: Oxford, 2015.

(5) Shaffer, P. T.; Metcalf, T. G.; Sproul, O. J. Chlorine resistance of poliovirus isolants recovered from drinking water. *Water Res.* **1980**, *40* (6), 1115−1121.

(6) Payment, P.; Tremblay, M.; Trudel, M. Relative resistance to chlorine of poliovirus and coxsackievirus isolates from environmental sources and drinking water. *Appl. Environ. Microbiol.* **1985**, *49* (4), 981−983.

(7) Ridgway, H. F.; Olson, B. H. Chlorine resistance patterns of bacteria from two drinking water distribution systems. *Appl. Environ. Microbiol.* **1982**, *44* (4), 972−987.

(8) Sun, W.; Liu, W.; Cui, L.; Zhang, M.; Wang, B. Characterization and identification of a chlorine-resistant bacterium, Sphingomonas TS001, from a model drinking water distribution system. *Sci. Total Environ.* **2013**, *458*−*460*, 169−175.

(9) Holland, J.; Spindler, K.; Horodyski, F.; Grabau, E.; Nichol, S.; Vandepol, S. Rapid Evolution of RNA Genomes. *Science* **1982**, *215* (26), 1577−1585.

(10) *Waterborne Pathogens AWWA Manual M48*, 2nd ed.; American Water Works Association: Denver, 2006.

(11) Duffy, S.; Shackelton, L. A.; Holmes, E. C. Rates of evolutionary change in viruses: patterns and determinants. *Nat. Rev. Genet.* **2008**, *9* (4), 267−276.

(12) Hijnen, W. A. M.; Schijven, J. F.; Bonné, P.; Visser, A.; Medema, G. J. Elimination of viruses, bacteria and protozoan oocysts by slow sand filtration. *Water Sci. Technol.* **2004**, *50* (1), 147−154.

(13) Maillard, J.-Y.; Hann, A. C.; Perrin, R. Resistance of Pseudomonas aeruginosa PAO1 phage F116 to sodium hypochlorite. *J. Appl. Microbiol.* **1998**, *85* (5), 799−806.

(14) McBride, R. C.; Ogbunugafor, C. B.; Turner, P. E. Robustness promotes evolvability of thermotolerance in an RNA virus. *BMC Evol. Biol.* **2008**, *8*, 231.

(15) Zhong, Q.; Carratalà, A.; Nazarov, S.; Guerrero-Ferreira, R. C.; Piccinini, L.; Bachmann, V.; Leiman, P. G.; Kohn, T. Genetic, structural, and phenotypic properties of MS2 coliphage with resistance to ClO_2 disinfection. *Environ. Sci. Technol.* **2016**, *50* (24), 13520−13528.

(16) Sedmak, G.; Bina, D.; MacDonald, J. Assessment of an enterovirus sewage surveillance system by comparison of clinical isolates with sewage isolates from Milwaukee, Wisconsin, collected August 1994 to December 2002. *Appl. Environ. Microbiol.* **2003**, *69* (12), 7181−7187.

(17) Gantzer, C.; Maul, A.; Audic, J. M.; Schwartzbrod, L. Detection of infectious enteroviruses, enterovirus genomes, somatic coliphages, and Bacteroides fragilis phages in treated wastewater. *Appl. Environ. Microbiol.* **1998**, *64* (11), 4307−4312.

(18) Okoh, A. I.; Sibanda, T.; Gusha, S. S. Inadequately treated wastewater as a source of human enteric viruses in the environment. *Int. J. Environ. Res. Public Health* **2010**, *7* (6), 2620−2637.

(19) Lodder, W. J.; de Roda Husman, A. M. Presence of noroviruses and other enteric viruses in sewage and surface waters in The Netherlands. *Appl. Environ. Microbiol.* **2005**, *71* (3), 1453−1461.

(20) Ahmad, T.; Zahid, S.; Ashraf, M. Detection of polio virus in municipal water bodies of Lahore, Pakistan. *Int. J. Biosci., Biochem. Bioinf.* **2013**, *3* (2), 157−160.

(21) Ehlers, M. M.; Grabow, W. O. K.; Pavlov, D. N. Detection of enteroviruses in untreated and treated drinking water supplies in South Africa. *Water Res.* **2005**, *39* (11), 2253−2258.

(22) Borchardt, M. a.; Spencer, S. K.; Kieke, B. a.; Lambertini, E.; Loge, F. J. Viruses in nondisinfected drinking water from municipal wells and community incidence of acute gastrointestinal illness. *Environ. Health Perspect.* **2012**, *120* (9), 1272−1279.

(23) Lodder, W. J.; Van Den Berg, H. H. J. L.; Rutjes, S. a.; De Roda Husman, a. M. Presence of enteric viruses in source waters for drinking water production in the Netherlands. *Appl. Environ. Microbiol.* **2010**, *76* (17), 5965−5971.

(24) *The Picornaviruses*; Ehrenfeld, E., Domingo, E., Roos, R. P., Eds.; American Society of Microbiology: Washington, DC, 2010.

(25) *Fields Virology*, 5th ed..; Knipe, D. M., Howley, P. M., Eds.; Lippincott Williams & Wilkins: Philadelphia, 2007.

(26) Bergelson, J. M.; Chan, M.; Solomon, K. R.; John, N. F. S. T.; Lin, H.; Finberg, R. W. Decay-accelerating factor (CD55), a glycosylphosphatidylinositol-anchored complement regulatory protein, is a receptor for several echoviruses. *Proc. Natl. Acad. Sci. U. S. A.* **1994**, *91*, 6245−6248.

(27) Bergelson, J. M.; Chan, M.; Solomon, K. R., St; John, N. F.; Lin, H.; Finberg, R. W. Decay-accelerating factor (CD55), a glycosylphosphatidylinositol-anchored complement regulatory protein, is a receptor for several echoviruses. *Proc. Natl. Acad. Sci. U. S. A.* **1994**, *91* (13), 6245−6248.

(28) Ward, T.; Powell, R. M.; Pipkin, P. A.; Evans, D. J.; Minor, P. D.; Almond, J. W. Role for β2-microglobulin in echovirus Infection of rhabdomyosarcoma cells. *J. Virol.* **1998**, *72* (7), 5360−5365.

(29) Chevaliez, S.; Balanant, J.; Maillard, P.; Lone, Y. C.; Lemonnier, F. a.; Delpeyroux, F. Role of class I human leukocyte antigen molecules in early steps of echovirus infection of rhabdomyosarcoma cells. *Virology* **2008**, *381* (2), 203−214.
(30) Kim, C.; Bergelson, J. M. Echovirus 7 entry into polarized intestinal epithelial cells requires clathrin and Rab7. *mBio* **2012**, *3* (2), 1−10.
(31) Xing, L.; Huhtala, M.; Pietiäinen, V.; Käpylä, J.; Vuorinen, K.; Marjomäki, V.; Heino, J.; Johnson, M. S.; Hyypiä, T.; Cheng, R. H. Structural and functional analysis of integrin alpha2I domain interaction with echovirus 1. *J. Biol. Chem.* **2004**, *279* (12), 11632−11638.
(32) Krieger, S. E.; Kim, C.; Zhang, L.; Marjomaki, V.; Bergelson, J. M. Echovirus 1 entry into polarized Caco-2 cells depends on dynamin, cholesterol, and cellular factors associated with macropinocytosis. *J. Virol.* **2013**, *87* (16), 8884−8895.
(33) Brandenburg, B.; Lee, L. Y.; Lakadamyali, M.; Rust, M. J.; Zhuang, X.; Hogle, J. M. Imaging poliovirus entry in live cells. *PLoS Biol.* **2007**, *5* (7), 1543−1555.
(34) Dahllund, L. The genome of echovirus 11. *Virus Res.* **1995**, *35*, 215−222.
(35) Zoni, R.; Zanelli, R.; Riboldi, E.; Bigliardi, L.; Sansebastiano, G. Investigation on virucidal activity of chlorine dioxide. experimental data on feline calicivirus, HAV and Coxsackie B5. *J. Prev. Med. Hyg.* **2007**, *48* (3), 91−95.
(36) Thurston-Enriquez, J. A.; Haas, C. N.; Jacangelo, J.; Gerba, C. P. Inactivation of enteric adenovirus and feline calicivirus by chlorine dioxide. *Appl. Environ. Microbiol.* **2005**, *71* (6), 3100−3105.
(37) Xue, B.; Jin, M.; Yang, D.; Guo, X.; Chen, Z.; Shen, Z.; Wang, X.; Qiu, Z.; Wang, J.; Zhang, B.; et al. Effects of chlorine and chlorine dioxide on human rotavirus infectivity and genome stability. *Water Res.* **2013**, *47* (10), 3329−3338.
(38) Alvarez, M. E.; Brien, R. T. O. Mechanisms of inactivation of poliovirus by chlorine dioxide and iodine. *Appl. Environ. Microbiol.* **1982**, *44* (5), 1064−1071.
(39) Wigginton, K. R.; Pecson, B. M.; Sigstam, T.; Bosshard, F.; Kohn, T. Virus inactivation mechanisms: impact of disinfectants on virus function and structural integrity. *Environ. Sci. Technol.* **2012**, *46* (21), 12069−12078.
(40) Li, J. W.; Xin, Z. T.; Wang, X. W.; Zheng, J. L.; Chao, F. H. Mechanisms of inactivation of hepatitis A virus in water by chlorine dioxide. *Water Res.* **2004**, *38* (6), 1514−1519.
(41) Jin, M.; Shan, J.; Chen, Z.; Guo, X.; Shen, Z.; Qiu, Z.; Xue, B.; Wang, Y.; Zhu, D.; Wang, X.; et al. Chlorine dioxide inactivation of enterovirus 71 in water and its impact on genomic targets. *Environ. Sci. Technol.* **2013**, *47* (9), 4590−4597.
(42) Simonet, J.; Gantzer, C. Degradation of the Poliovirus 1 genome by chlorine dioxide. *J. Appl. Microbiol.* **2006**, *100* (4), 862−870.
(43) Jin, M.; Zhao, Z.; Wang, X.; Shen, Z.; Xu, L.; Yu, Y.; Qiu, Z.; Zhaoli, C.; Wang, J.; Aihua, H.; et al. The 40−80 nt Region in the 50-NCR of genome is a critical target for inactivating poliovirus by chlorine dioxide. *J. Med. Virol.* **2012**, *84*, 526−535.
(44) Alvarez, M. E.; O'Brien, R. T. Mechanisms of inactivation of poliovirus by chlorine dioxide and iodine. *Appl. Environ. Microbiol.* **1982**, *44* (5), 1064−1071.
(45) Haas, C. N.; Joffe, J. Disinfection under dynamic conditions: modification of Hom's model for decay. *Environ. Sci. Technol.* **1994**, *28* (7), 1367−1369.
(46) Fletcher, I. J.; Hemmings, P. Determination of chlorine dioxide in potable waters using chlorophenol red. *Analyst* **1985**, *110* (6), 695−699.
(47) Triantafilou, M.; Wilson, K. M.; Triantafilou, K. Identification of echovirus 1 and coxsackievirus A9 receptor molecules via a novel flow cytometric quantificationqMethod. *Cytometry* **2001**, *43* (4), 279−289.
(48) Haas, C. N.; Rose, J. B.; Gerba, C. P. *Quantitative Microbial Risk Assessment*, 2nd ed.; John Wiley & Sons, Inc.: Hoboken, 2014.
(49) Sigstam, T.; Rohatschek, A.; Zhong, Q.; Brennecke, M.; Kohn, T. On the cause of the tailing phenomenon during virus disinfection by chlorine dioxide. *Water Res.* **2013**, *48* (1), 82−89.
(50) Ciota, A. T.; Lovelace, A. O.; Ngo, K. A.; Le, A. N.; Maffei, J. G.; Franke, M. A.; Payne, A. F.; Jones, S. A.; Kauffman, E. B.; Kramer, L. D. Cell-specific adaptation of two flaviviruses following serial passage in mosquito cell culture. *Virology* **2007**, *357* (2), 165−174.
(51) Zaini, Z.; Phuektes, P.; McMinn, P. A reverse genetic study of the adaptation of human enterovirus 71 to growth in Chinese hamster ovary cell cultures. *Virus Res.* **2012**, *165* (2), 151−156.
(52) Simmonds, P.; Tuplin, A.; Evans, D. J. Detection of genome-scale ordered RNA structure (GORS) in genomes of positive-stranded RNA viruses: Implications for virus evolution and host persistence. *RNA* **2004**, *10* (9), 1337−1351.
(53) Smith, J. M.; Haigh, J. The hitch-hiking effect of a favorable gene. *Genet. Res.* **1974**, *23* (1), 23−35.
(54) Bank, C.; N, R.; Liu, P.; Matuszewski, S.; Shim, H.; Foll, M.; Bolon, D. N.; Zeldovich, K. B.; Kowalik, T. F.; Finberg, R. W.; et al. An experimental evaluation of drug induced mutational meltdown as an antiviral treatment strategy. *Evolution* **2016**, *70* (11), 2470−2484.
(55) Stuart, A. D.; McKee, T. a; Williams, P. a; Harley, C.; Shen, S.; Stuart, D. I.; Brown, T. D. K.; Lea, S. M. Determination of the structure of a decay accelerating factor-binding clinical isolate of echovirus 11 allows mapping of mutants with altered receptor requirements for infection. *J. Virol.* **2002**, *76* (15), 7694−7704.
(56) Rezaikin, A. V.; Novoselov, A. V.; Sergeev, A. G.; Fadeyev, F. a.; Lebedev, S. V. Two clusters of mutations map distinct receptor-binding sites of echovirus 11 for the decay-accelerating factor (CD55) and for canyon-binding receptors. *Virus Res.* **2009**, *145*, 74−79.
(57) Lea, S. M.; Powell, R. M.; McKee, T.; Evans, D. J.; Brown, D.; Stuart, D. I.; Van Der Merwe, P. A. Determination of the affinity and kinetic constants for the interaction between the human virus echovirus 11 and its cellular receptor, CD55. *J. Biol. Chem.* **1998**, *273* (46), 30443−30447.
(58) McDermott, B. M.; Rux, A. H.; Eisenberg, R. J.; Cohen, G. H.; Racaniello, V. R. Two distinct binding affinities of poliovirus for its cellular receptor. *J. Biol. Chem.* **2000**, *275* (30), 23089−23096.
(59) Xing, L.; Tjarnlund, K.; Lindqvist, B.; Kaplan, G. G.; Feigelstock, D.; Cheng, R. H.; Casasnovas, J. M. Distinct cellular receptor interactions in poliovirus and rhinoviruses. *EMBO J.* **2000**, *19* (6), 1207−1216.
(60) Strauss, M.; Filman, D. J.; Belnap, D. M.; Cheng, N.; Noel, R. T.; Hogle, J. M. Nectin-like interactions between poliovirus and its receptor trigger conformational changes associated with cell entry. *J. Virol.* **2015**, *89* (8), 4143−4157.
(61) Belnap, D. M.; McDermott, B. M.; Filman, D. J.; Cheng, N.; Trus, B. L.; Zuccola, H. J.; Racaniello, V. R.; Hogle, J. M.; Steven, a C. Three-dimensional structure of poliovirus receptor bound to poliovirus. *Proc. Natl. Acad. Sci. U. S. A.* **2000**, *97* (1), 73−78.
(62) He, Yongning; Chipman, Paul R.; Howitt, Jason; Bator, Carol M.; Whitt, Michael A.; Baker, Timothy S.; Kuhn, Richard J.; Anderson, Carl W.; Freimuth, P. R. M. G. Interaction of coxsackievirus B3 with the full length coxsackievirus-adenovirus receptor. *Nat. Struct. Biol.* **2001**, *8* (10), 874−878.
(63) De Palma, A. M.; Vliegen, I.; De Clercq, E.; Neyts, J. Selective inhibitors of picornavirus replication. *Med. Res. Rev.* **2008**, *28* (6), 823−884.
(64) Schmidtke, M.; Hammerschmidt, E.; Schüler, S.; Zell, R.; Birch-Hirschfeld, E.; Makarov, V. A.; Riabova, O. B.; Wutzler, P. Susceptibility of coxsackievirus B3 laboratory strains and clinical isolates to the capsid function inhibitor pleconaril: Antiviral studies with virus chimeras demonstrate the crucial role of amino acid 1092 in treatment. *J. Antimicrob. Chemother.* **2005**, *56* (4), 648−656.
(65) Ledford, R. M.; Collett, M. S.; Pevear, D. C. Insights into the genetic basis for natural phenotypic resistance of human rhinoviruses to pleconaril. *Antiviral Res.* **2005**, *68* (3), 135−138.
(66) Benschop, K. S. M.; Wildenbeest, J. G.; Koen, G.; Minnaar, R. P.; Van Hemert, F. J.; Westerhuis, B. M.; Pajkrt, D.; Van Den Broek, P. J.; Vossen, A. C. T. M.; Wolthers, K. C. Genetic and antigenic structural characterization for resistance of echovirus 11 to pleconaril in an immunocompromised patient. *J. Gen. Virol.* **2015**, *96* (3), 571−579.

DOI: 10.1021/acs.est.7b03288
Environ. Sci. Technol. 2017, 51, 10746−10755

(67) Sobo, K.; Rubbia-Brandt, L.; Brown, T. D. K.; Stuart, A. D.; McKee, T. a. Decay-accelerating factor binding determines the entry route of echovirus 11 in polarized epithelial cells. *J. Virol.* **2011**, *85* (23), 12376−12386.
(68) Stuart, A. D.; Eustace, H. E.; Mckee, T. A.; Brown, T. D. K. A Novel Cell Entry Pathway for a DAF-Using Human Enterovirus Is Dependent on Lipid Rafts. *J. Virol.* **2002**, *76* (18), 9307−9322.
(69) Marjoma, V.; Upla, P.; Pelkmans, L. Echovirus 1 endocytosis into caveosomes requires lipid rafts, dynamin II, and signaling events. *Mol. Biol. Cell* **2004**, *15*, 4911−4925.
(70) Taylor, M. P.; Koyuncu, O. O.; Enquist, L. W. Subversion of the actin cytoskeleton during viral infection. *Nat. Rev. Microbiol.* **2011**, *9* (6), 427−439.
(71) Sobo, K.; Stuart, A. D.; Rubbia-Brandt, L.; Brown, T. D. K.; McKee, T. a. Echovirus 11 infection induces dramatic changes in the actin cytoskeleton of polarized Caco-2 cells. *J. Gen. Virol.* **2012**, *93* (Pt 3), 475−487.
(72) Upla, P.; Marjoma, V.; Kankaanpa, P.; Ivaska, J.; Goot, F. G. Van Der; Heino, J. Clustering Induces a Lateral Redistribution of alpha2beta1 Integrin from Membrane Rafts to Caveolae and Subsequent Protein Kinase C − dependent Internalization. *Mol. Biol. Cell* **2004**, *15*, 625−636.
(73) Yea, C.; Dembowy, J.; Pacione, L.; Brown, M. Microtubule-Mediated and Microtubule-Independent Transport of Adenovirus Type 5 in HEK293 Cells. *J. Virol.* **2007**, *81* (13), 6899−6908.
(74) USEPA. *Disinfection Profiling and Benchmarking Guidance Manual*; Washington, D.C., 1999.
(75) Stuart, A. D.; Mckee, T. A.; Williams, P. A.; Harley, C.; Shen, S.; Stuart, D. I.; Brown, T. D. K.; Lea, S. M. Determination of the Structure of a Decay Accelerating Factor-Binding Clinical Isolate of Echovirus 11 Allows Mapping of Mutants with Altered Receptor Requirements for Infection. *J. Virol.* **2002**, *76* (15), 7694−7704.

DOI: 10.1021/acs.est.7b03288
Environ. Sci. Technol. 2017, 51, 10746−10755